Combined Orbital Floor and Medial Wall Fractures Involving the Inferomedial Strut: Repair Technique and Case Series Using Preshaped Porous Polyethylene/Titanium Implants

Raymond I. Cho, MD, FACS[1] Brett W. Davies, MD[2]

[1] Oculoplastic and Orbital Surgery Service, San Antonio Military Medical Center
[2] Department of Ophthalmology, Wilford Hall Ambulatory Surgical Center, San Antonio, Texas

Address for correspondence Raymond I. Cho, MD, FACS, Department of Ophthalmology, Walter Reed National Military Medical Center, 8901 Rockville Pike, Bethesda, MD (e-mail: raymond.cho@us.army.mil).

Craniomaxillofac Trauma Reconstruction 2013;6:161–170

Abstract

Background Combined orbital floor and medial wall fractures can be technically challenging to repair, particularly when the inferomedial strut is involved. A surgical repair technique is described utilizing a single preshaped porous polyethylene/titanium implant to span both defects.

Methods Retrospective interventional case series.

Results Fracture repair was performed on 17 orbits (16 patients) between October 2009 and February 2012. Subsequent surgical revision was required in three cases (18%). Visual acuity was stable or improved in all cases. Of 7 patients with preoperative diplopia, 5 improved and 2 remained stable postoperatively, and there were no cases of new or worsened diplopia following surgery. Postoperative asymmetry in Hertel exophthalmometry averaged 1.0 mm (range 0 to 2 mm). Preoperatively, average orbital volume was 122.7% compared with control (range 109 to 147%, standard deviation [SD] 9.6), which improved to 100.3% postoperatively (range 92 to 110%, SD 5.7). The average decrease in orbital volume was 22.5% (range 10 to 54%, SD 11.4, $p < 0.001$).

Conclusions With careful preoperative planning and meticulous surgical technique, combined orbital floor and medial wall fractures involving the inferomedial strut can be successfully repaired with a preshaped porous polyethylene/titanium implant through a transconjunctival/transcaruncular approach with inferior oblique disinsertion.

Keywords
- orbital fracture
- orbital floor
- medial wall
- inferomedial strut
- porous polyethylene
- titanium

The most commonly fractured walls of the orbit are the floor and medial wall, and repair is indicated in cases of extraocular muscle entrapment, diplopia, globe malposition, and significant orbital volume expansion.[1–5] Combined fractures of the floor and medial wall are more likely than isolated orbital wall fractures to require treatment due to increased volume expansion; they are often associated with compromise of the inferomedial strut at the ethmoid-maxillary junction (►**Fig. 1**). The large size of these fractures and the loss of internal bony support can make surgical repair particularly challenging. Several techniques have been described to deal with this fracture pattern using a variety of implant materials

received
August 29, 2012
accepted
September 14, 2012
published online
May 31, 2013

DOI http://dx.doi.org/10.1055/s-0033-1343785.
ISSN 1943-3875.

Figure 1 The inferomedial strut (arrows), shown in coronal computed tomography scan images of two different patients with combined orbital floor/medial wall fractures. Intact left strut (A), and fractured/displaced strut (B).

and surgical approaches.[6–10] However, the goal of restoring the normal contours of the bony orbit while avoiding postoperative complications remains difficult to achieve. We herein describe a repair technique and report a case series using preshaped porous polyethylene (PPE)/titanium implants through a combined transconjunctival and transcaruncular approach with disinsertion of the inferior oblique muscle.

Methods

Institutional Review Board approval was obtained for this study. A retrospective review was conducted of all cases of combined orbital floor/medial wall fracture repair performed by the senior author (R.I.C.) between October 2009 and February 2012. Cases utilizing the technique as described below were included. Exclusion criteria included lack of postoperative imaging or follow-up. Outcome measures included visual acuity, diplopia, Hertel exophthalmometry, and symmetry of orbital volume. Preoperative Hertel measurements were not included in the analysis, because a majority of patients had confounding orbital edema or hemorrhage as a result of the initial trauma. Postoperative Hertel measurements were recorded at the last available follow-up visit, and were excluded in anophthalmic patients. Pre- and postoperative orbital volume symmetry was determined by analyzing coronal computed tomography (CT) scan images using Abode Photoshop Elements 8.0 (Adobe Systems Inc., San Jose, CA). At sequential 2-mm intervals, the lasso tool was used to trace the orbital outline on each side, and the number of incorporated pixels shown in the histogram view was recorded. The total pixel count from all images was calculated on each side, and the number on the surgical side was divided by the uninjured (control) side. For patients with bilateral fractures, the control outline was carefully drawn to replicate normal orbital anatomy as closely as possible. Volume of the surgical orbit was expressed as a percentage of the control (e.g., 110% represents a 10% expansion of volume). Statistical analysis of orbital volumes was performed using the Wilcoxon signed rank test.

Surgical Technique

Preoperative planning included detailed measurements taken from the orbital CT scan using the caliper function on the hospital's imaging system to determine the size and shape of the implant (►**Fig. 2**). Coronal measurements were used to determine the width of the floor and medial wall components; the axial and sagittal measurements dictated the anterior-to-posterior length of the medial wall and floor, respectively. The flex point between the floor and medial portions of the implant approximated the position of

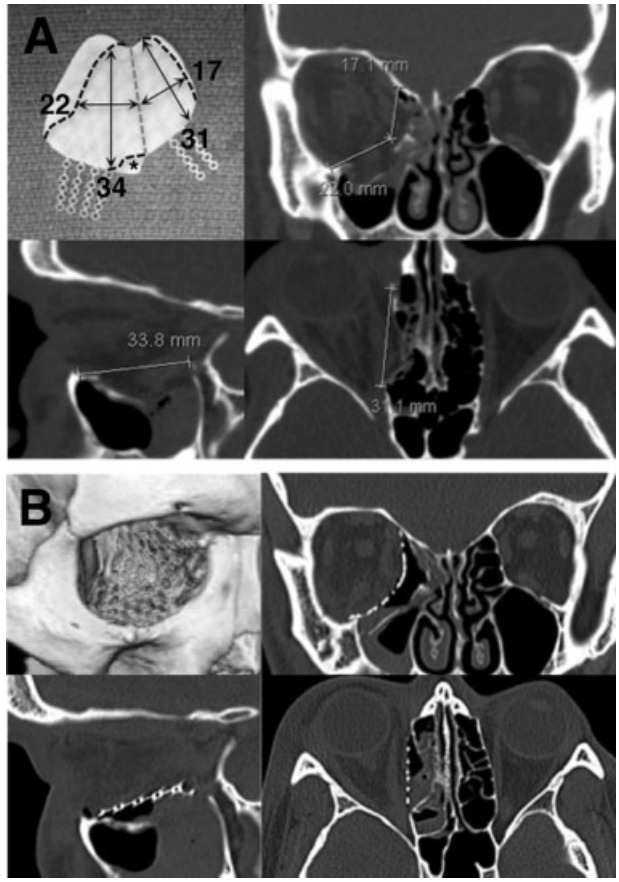

Figure 2 (A) Preoperative computed tomography measurements were taken in all three imaging planes at multiple levels to determine the implant dimensions (single cuts shown here). Note that the axial measurement of the medial wall begins behind the posterior lacrimal crest. Top left, the orbital floor/wall implant with black dashed lines showing areas to be trimmed, and a gray dashed line showing the planned flexure point between the floor and medial wall. Area marked with asterisk (*) is trimmed to make room for the nasolacrimal duct and inferior oblique origin. (B) Postoperative computed tomography scan images and three-dimensional reconstruction showing implant placement in the same patient.

inferomedial strut on the uninjured side. All implant measurements took into account the need for a sufficient amount of overlap over the bony ledges. Serial measurements were taken at set image intervals for each case, typically every 4 to 5 mm.

All cases were performed under general anesthesia. Forced duction testing was performed at the beginning of the case to document any preoperative globe restriction. Following the injection of local infiltration anesthesia, a lateral canthotomy and inferior cantholysis was performed with tenotomy scissors. A transconjunctival incision was created through the inferior fornix with Westcott scissors or needle cautery on a low pure cut setting. Dissection was carried through the retractors to the inferior orbital rim, where the periosteum was opened with needle cautery, and subperiosteal dissection carried into the orbit and across the orbital floor with periosteal elevators. All prolapsed orbital soft tissues were carefully reduced from the fracture site and bony ledges identified laterally and posteriorly.

Attention was turned to the medial orbit, where an incision was created with Westcott scissors between the caruncle and plica semilunaris, and extended inferiorly to join the fornix incision. Blunt tenotomy scissors were placed through the transcaruncular incision at a 45-degree posteromedial angle, palpating the medial wall behind the posterior lacrimal crest, and spread to expose the medial wall. Jameson muscle hooks and malleable ribbon retractors were used to retract the conjunctiva and orbital fat. The periosteum behind the posterior lacrimal crest was opened with a bent crescent blade or needle cautery, and subperiosteal dissection was carried along the medial wall, reducing the orbital contents and identifying the superior and posterior ledges of the fracture. The anterior and/or posterior ethmoidal neurovascular bundles were cauterized and divided to fully expose the superior ledge of bone and allow for proper seating of the implant.

The inferior and medial dissections were joined to create a single dissection plane. The origin of the inferior oblique muscle was identified just behind the inferomedial orbital rim and disinserted from the bone with a periosteal elevator. The remaining bridge of soft tissue and periosteum separating the inferior and medial incisions was sharply divided, providing maximal surgical exposure and access to the inferomedial orbit. Great care was taken during this maneuver to avoid damage to the lacrimal sac, which lies just medial to the inferior oblique origin.

The implant material used in all cases was a preshaped PPE-imbedded titanium mesh implant specifically designed for orbital floor and medial wall reconstruction (Medpor Titan OFW, Stryker, Kalamazoo, MI). The implant was soaked in antibiotic solution and trimmed to the predetermined dimensions. It was then bent to conform to the natural bony contours of the orbit (►**Fig. 3**), reproducing the upward posteromedial slope of the floor, the anterior-to-posterior s-shaped curvature, and the ~ 120- to 130-degree angle between the floor and medial wall. With the orbital contents retracted and bony ledges exposed by ribbon retractors, the implant was placed within the subperiosteal space to cover the defect. Care was taken to ensure that the edges of the implant rested securely on stable bony ledges, and that no orbital soft tissue was incarcerated beneath the implant. Forced duction testing was repeated to confirm normal globe mobility. The anterior titanium extensions of the implant were then secured to the inferolateral rim and frontal process of the maxilla with titanium screws. In most cases, only two of the extensions were fixated (laterally and superomedially), and the remainder were broken off and discarded. The lateral canthal tendon was resuspended from the periosteum behind the lateral orbital rim with a 4–0 polydioxanone suture, and the conjunctiva was closed with buried interrupted 6–0 plain gut sutures.

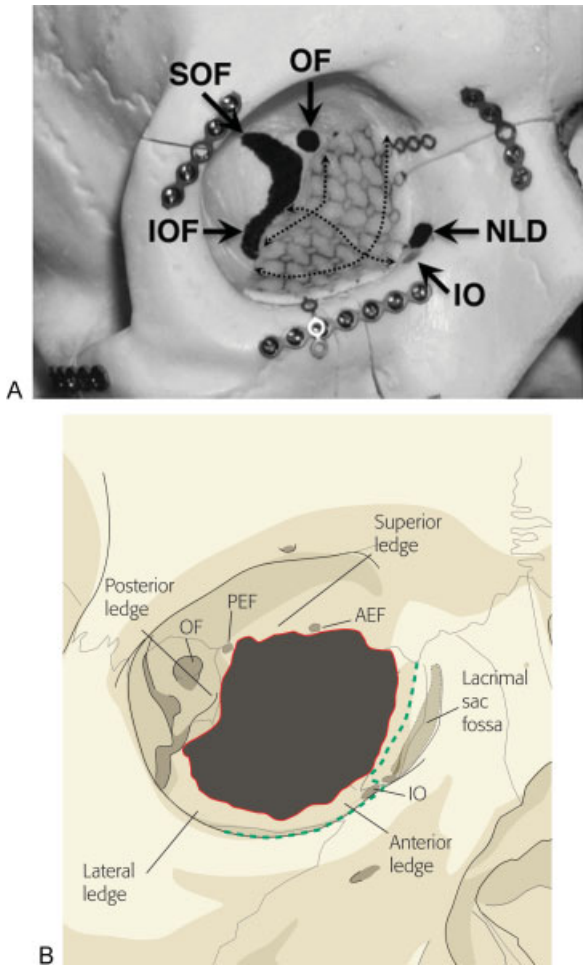

Figure 3 (A) Trimmed orbital floor/wall implant positioned within model right orbit, showing its relationship with major orbital landmarks. Dashed lines demonstrate the contours of the implant, replicating those of the orbital floor and medial wall. (B) Illustration of floor/medical wall fracture showing key bony support ledges. Green dashed line represents periosteal incision. Abbreviations: AEF, anterior ethmoidal foramen; IO, inferior oblique muscle origin; IOF, inferior orbital fissure; NLD, nasolacrimal duct; OF, optic foramen; PEF, posterior ethmoidal foramen; SOF, superior orbital fissure.

Results

During the study period, 19 orbits of 18 patients with combined orbital floor and medial wall fractures involving the inferomedial strut underwent the procedure described

earlier. Two were excluded due to lack of postoperative imaging, leaving a total of 17 cases (16 patients). Twelve patients (75%) were male, and the average age was 30 (range 21 to 54). Eight patients (50%) were referred from other surgical services for complications following initial fracture repair. Four patients were U.S. service members wounded during combat operations in Iraq or Afghanistan. Concomitant craniofacial injuries were common, with 13 patients (81%) requiring repair of facial buttress or skull base fractures. Ocular injuries were also common, with three patients requiring enucleation following open globe repair, three sustaining choroidal ruptures, and one suffering traumatic optic neuropathy with no light perception. All initial repairs except one were performed within 1 month of the injury (average 9.3 days, range 1 to 24). The single outlier (case 17) underwent initial repair 5 years postinjury.

Surgical outcomes are summarized in ►**Table 1**. Of the 17 cases performed by the senior author, three (18%) required subsequent surgical revision—two due to inadequate reduction, and one due to presumed compressive optic neuropathy (postoperative afferent pupillary defect in an intubated patient). This same patient (case 11) expired in the postoperative period due to multisystem organ failure following extensive burn injuries. Visual acuity improved or remained within one line of preoperative vision in all other cases. There were no cases of new or worsened diplopia following surgery, and five of seven patients with preoperative diplopia (71%) improved or resolved postoperatively. One of the patients with persistent diplopia (case 1) was referred to us several months after primary repair and underwent final revision 18 months later. The other patient (case 6) was transferred to a long-term care facility 1 week postoperatively and was lost to follow-up.

Exophthalmometry measurements were excluded in four patients with acquired anophthalmos of the operative or fellow orbit, and were unavailable in two others. In the remaining 11 cases, the average asymmetry in postoperative Hertel measurements was 1 mm (range 0 to 2 mm). Analysis of preoperative CT scan imaging (►**Fig. 4**) revealed preoperative orbital volume expansion in all cases, with an average of 122.8% (range 108 to 147%, standard deviation [SD] 9.6). The average postoperative orbital volume was 100.3% of control (range 92 to 110%, SD 5.7), with an average postoperative decrease in orbital volume of 22.5% (range 10 to 54%, SD 11.4, $p < 0.001$).

Discussion

Combined orbital floor and medial wall fractures involving the inferomedial strut represent a unique technical challenge to the orbital surgeon. The anatomic significance of the strut has been discussed by several authors in the context of orbital decompression surgery,[11–13] but it has not garnered a great deal of attention in the orbital trauma literature. When the inferomedial strut is intact, it can be used to support separate implants placed over each of the fractures individually. However, when this support is compromised, the surgeon has essentially two choices: use multiple or modified implants to compensate for the loss of medial support; or use a single implant that is large enough to bridge the entire defect, from the medial roof to the lateral floor.

An example of the first approach was described by Su and Harris,[6] who used overlapping nylon foil implants to repair the floor and medial wall. However, the majority of the cases in their study did not involve the inferomedial strut, and the ones that did required the use of a third implant at the junction of the floor and medial wall implants. Another technique described by Choi et al uses two separate PPE channel implants (Medpor channel sheet, Stryker, Kalamazoo, MI), both of which are screw fixated to the orbital rim by titanium plates placed within the longitudinal channels.[7] The plates can be used to cantilever the implants into anatomic position in the absence of internal bony support. However, these implants are relatively thick (2.3 mm) and have the potential to cause postoperative hyperglobus.

The second approach—single-implant repair—has been described by several authors. Nunery at al reported the use of a "wraparound" nylon foil implant to repair these defects.[8] Although their results were excellent overall, only 14 of 102 cases involved the inferomedial strut. The use of such a flexible material to span these large defects raises the theoretical concern of implant buckling and displacement. Additionally, nylon foil's lack of malleability is problematic when attempting to replicate the normal contours of the floor and medial wall. Other reported single-implant techniques utilize titanium mesh plates, which are either individually preformed based on preoperative stereolithography or manufactured to replicate the bony contours of the floor and medial wall (Matrix Midface preformed orbital plate, Synthes Inc., West Chester, PA).[9,10] Although in theory, these implants, if placed properly, should produce excellent anatomic results, we avoid their use for two reasons. First, the size of the premanufactured implant is not large enough to completely cover many of the defects we encounter. The second reason is our own experience as well as that of other authors with orbital adherence syndrome caused by exposed titanium mesh in the orbit.[14]

The use of PPE-imbedded titanium for the repair of floor and medial wall fractures has been described by several authors,[15–19] but this to our knowledge is the first published report utilizing the preshaped orbital floor/wall implant designed by Holck (Medpor Titan OFW, Stryker, Kalamazoo, MI). This implant combines the capacity of PPE for fibrovascular ingrowth with the strength and malleability of titanium mesh, along with the additional benefits of a preshaped design and titanium extensions for screw fixation to the orbital rim. The size and shape of the implant is intended to provide coverage for the largest possible fractures, and requires trimming to fit most orbits (►**Fig. 2**). It is currently available in three versions: porous on both sides (MTM), nonporous (barrier) on both sides, or a combination (MTB) with the barrier surface placed on the orbital side to prevent soft tissue adherence. The MTB version was used in all cases but one where an MTM implant was used, and this case is discussed below.

Table 1 Clinical information and outcome measures

Case	Orbit	Cause of injury	No. of repair attempts	Associated injuries/procedures	Follow-up interval (wk)	Preoperative vision	Postoperative vision	Postoperative diplopia	Hertel asymmetry (mm)[d]
1	L	Blast	3[a]	R NOE, CR OD, cataract OD	1	HM	20/70	Stable	NA
2	R	Assault	2[a]	B NOE/LeFort 1/mandible, L ZMC	14	NA	20/20	None	NA
3	L	MVA	1	B ZMC/FS	7	20/20	20/25	None	−1
4	R	Assault	1	None	5	20/40	20/25	Improved	+2
5	L	MVA	2[a]	B ZMC	1	20/70	20/25	Improved	−1
6	R	GSW	1	B FS, R NOE/roof/mandible, CR OD	1	CF 2 ft	8/200	Stable	0
7	R[c]	Assault	1	B NOE, enucleation OD, L ZMC, CR OS	3	NLP	[b]	[b]	[b]
8	L[c]	Assault	1	B NOE, enucleation OD, L ZMC, CR OS	3	20/400	20/400	[b]	[b]
9	L	MVA	2[a]	L ZMC/roof/NOE, B mandible, TON OS	31	NLP	NLP	[b]	−2
10	R	MVA	1	B ZMC/NOE/FS	8	NA	20/25	None	−2
11	R	Plane crash	2	B NOE/FS, R ZMC, 70% burns (expired)	7	NA	NA	NA	0
12	L	Assault	2[a]	L ZMC	49	20/30	20/20	Improved	−1
13	R	Assault	2[a]	None	22	20/25	20/25	Improved	0
14	R	Blast	1	R ZMC, enucleation OD	14	[b]	[b]	[b]	[b]
15	L	Blast	3[a]	B LeFort 1, R orbital floor/medial wall	16	20/80	20/25	Improved	−1
16	L	Assault	1	None	10	20/30	20/20	None	−0.5
17	R	GSW	2[a]	R ZMC, enucleation OD	7	[b]	[b]	[b]	[b]

Abbreviations: B, bilateral; CF, count fingers; CR, choroidal rupture; OD, oculus dexter; OS, oculus sinister; FS, frontal sinus fracture; GSW, gunshot wound; HM, hand motion; L, left; MVA, motor vehicle accident; NA, not available; NLP, no light perception; NOE, naso-orbital-ethmoid fracture; R, right; TON, traumatic optic neuropathy; ZMC, zygomaticomaxillary complex fracture.

[a]Initial repair performed by referring service.

[b]Data excluded due to blindness or anophthalmos.

[c]Fellow orbits of same patient.

[d]Positive value indicates relative proptosis, negative value indicates relative enophthalmos

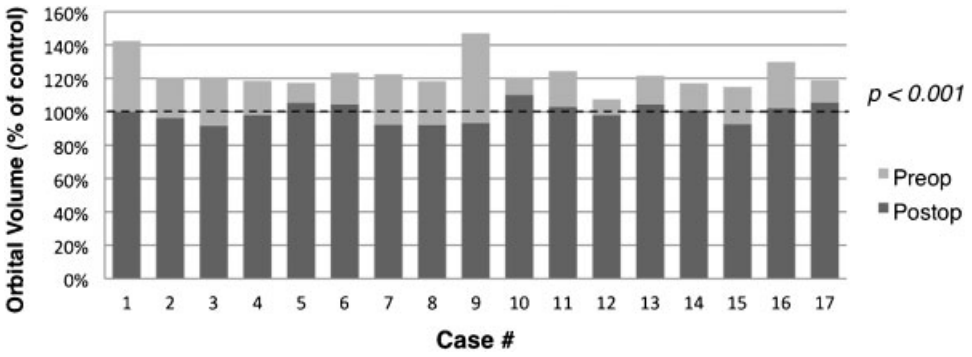

Figure 4 Preoperative versus final postoperative orbital volumes, expressed as a percentage of the control orbit.

When placing an implant of this size within the orbit, adequate surgical exposure and access are essential. The transconjunctival and transcaruncular incisions are both time-tested approaches to orbital fracture repair,[19–25] but neither incision alone is large enough to permit placement of this implant. When the two approaches are combined and the inferior oblique muscle disinserted, the entire surgical field becomes beautifully exposed. Combined transconjunctival and transcaruncular orbitotomy has been previously described by several authors,[26–28] along with disinsertion of the inferior oblique by others.[7,17] The combination of these approaches has proven indispensable to us in the management of these challenging cases. Although some authors have advocated dividing the inferior oblique near its origin and reapproximating the muscle with sutures at the end of the case,[26] we have found that direct disinsertion obviates the need for sutures. Mild vertical and/or torsional diplopia can occasionally occur in the early postoperative period, but in our experience has always resolved within a week or two. Damage to the lacrimal sac is a potential, but entirely avoidable, complication of this approach, and it did not occur in any of our cases.

Proper implant sizing and shaping is critical to the success of this technique. Given the relatively large surface area of the implant, the rigidity of the material, and the close proximity of the implant to vital orbital structures, seemingly small deviations in contour and shape can potentially result in significant complications. Therefore, we highly recommend the use of preoperative CT scan measurements to determine the appropriate dimensions of the implant (►**Fig. 2**). When shaping the implant prior to insertion, careful attention must be paid to replicating the slopes and curves of the floor and medial wall,[29] and a thorough three-dimensional understanding of the complex anatomy of the bony orbit is an absolute prerequisite to using this technique (►**Fig. 3**).

Positioning of the implant on stable ledges of bone is also critical, as no implant, no matter how well designed or shaped, will serve its purpose if not placed anatomically. Anterior and lateral bony ledges are relatively easy to obtain, but the most important and most problematic support points are the posterior and superior ledges. Failure to support the implant on these ledges was implicated in all eight of the cases referred to us for revision (►**Fig. 5** and ►**Fig. 6**), as well as two of the three author's cases needing revision. Posterior floor and medial wall support are critical but often lacking, and many surgeons are loath to venture so far into the orbit for fear of injuring the optic nerve. However, meticulous planning, a solid knowledge of orbital anatomy, and the use of adjunctive surgical techniques can decrease this risk. Intraoperative measurements of orbital depth can be compared with preoperative CT scan measurements, and the posterior ethmoidal foramen can serve as a vital anatomic reference point relative to the optic nerve. Other potentially useful modalities include intraoperative CT scanning, surgical navigation devices, and sinus endoscopy (►**Fig. 7**). The superior ledge is also critical to proper implant placement and is usually found at the level of the frontoethmoid suture. An excellent way to verify the location of this landmark is to divide the anterior and posterior ethmoidal neurovascular bundles and continue dissecting subperiosteally to the medial orbital roof. Care must be taken not to mistake the fovea ethmoidalis for the orbital roof, particularly when the medial wall is displaced far into the ethmoid sinus.

Our revision rate of 18% reflects the high degree of difficulty in using this technique. The first revision (case 1) was required due to failure to place the medial edge of the implant on the superior ledge. Postoperative enophthalmos was evident despite the stacking of multiple implants over the floor implant. We have since abandoned the practice of implant stacking, maintaining that no amount of stacking can take the place of proper anatomic reduction. The second complication (case 11) was a presumed case of compressive optic neuropathy, and was corrected by implant repositioning. The third revision (case 15) also resulted from failure to find posterior and superior support, resulting in enophthalmos. In this case, an MTM implant was initially used due to unavailability of the MTB, and its relative lack of rigidity made positioning of the implant more difficult.

The results of this case series should be interpreted in the context of our study's limitations, which include its retrospective nature and the numerous concomitant injuries that potentially impacted our results. The fact that half of our patients were referred from other services following unsuccessful primary repair underscores the high degree of

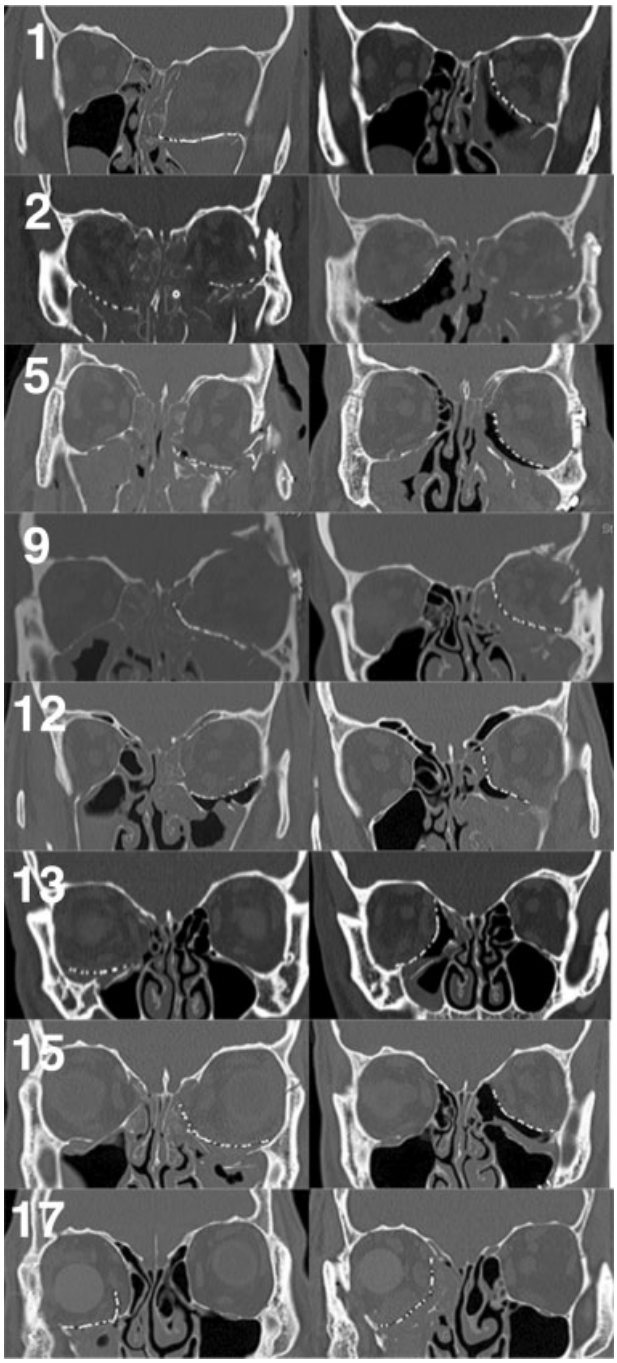

Figure 5 Preoperative (left) and final postoperative (right) coronal computed tomography scan images of all eight cases referred to the senior author for revision, with corresponding case numbers. Interim scans for cases 1 and 15 are not shown. Note that in case 2, the superior edge of the right orbital implant is not ideally positioned on the superior bony ledge. The left orbit of case 2 was not revised per the referring service's request.

complexity and difficulty in managing these cases. In some instances, incomplete reduction of facial buttress fractures resulted in orbital volume changes that could not be completely compensated by anatomic reconstruction of the floor and medial wall. Vision loss due to traumatic optic neuropathy or globe injury, motility disturbances caused by previously entrapped extraocular muscles or postsurgical scarring, and altered exophthalmometry measurements due to orbital edema/hemorrhage or displacement of the lateral rim also confounded analysis of these outcome measures. Despite these many variables, however, it is still notable that the average postoperative asymmetry in Hertel measurements was only 1 mm.

The difficulty in obtaining clinically useful exophthalmometry measurements led us to perform a more objective analysis of our reconstructive outcomes through the calculation of orbital volume symmetry. Our method of volume estimation is similar to those used in previous studies,[30–32] with the major difference being that we calculated relative instead of absolute volumes, which we felt would provide a more useful indication of orbital symmetry. As mentioned in our methods section, the presence in some cases of bilateral fractures made it necessary to alter the outline of the control orbit to replicate the normal anatomy. An additional challenge was accounting for the effects of head turn in the CT scanner, which sometimes placed coronal cuts at different anteroposterior levels on each side. We compensated for this by using major anatomic landmarks such as the optic foramen and superior orbital fissure to correspond to respective CT image cuts as closely as possible. Because all of our coronal series were obtained at intervals of 2 mm or less, the maximum theoretical offset between images was only 1 mm. Although the CT scan protocol was not standardized between patients, the fact that orbital volume percentages were calculated using fellow orbits in the same imaging series significantly reduces potential errors in our analysis. In light of these considerations, we believe that our overall orbital symmetry of 100.3% demonstrates that this technique can produce a reproducible anatomic reconstruction of the orbital floor and medial wall.

An additional limitation of this study is the relatively short follow-up interval for some of our cases. This is a frequent issue for civilian trauma patients at our institution, many of whom are indigent, noncompliant, travel long distances for care, and may have limited eligibility for care due to government regulations. It is impossible to predict whether longer follow-up periods would have altered outcome measures such as visual acuity, diplopia, or Hertel measurements. However, we maintain that the anatomic outcomes as documented by postoperative CT scanning are unlikely to change in any significant way, regardless of the follow-up interval.

The findings of our study underscore several important points. First, the amount of force required to fracture the inferomedial strut is significant, and often results in concomitant injuries to the facial buttresses, skull base, and ocular structures. Second, when treating fractures of this nature, it can be extremely beneficial to both patients and surgeons to utilize a multidisciplinary approach, involving a combination of oculoplastic surgery, otolaryngology, oral maxillofacial surgery, and/or general plastic surgery. Finally, this procedure can be extremely challenging to perform correctly, and an intimate familiarity with orbital anatomy is absolutely critical to ensuring satisfactory outcomes. Careful preoperative planning and meticulous surgical technique are also important elements of success.

Figure 6 Case 9. (A, B) Before and (C, D) 5 months after left orbital fracture revision, midface lift, and lateral canthopexy, followed by staged left superior rectus recession and left upper lid internal ptosis repair. See Fig. 5 for corresponding computed tomography scan images.

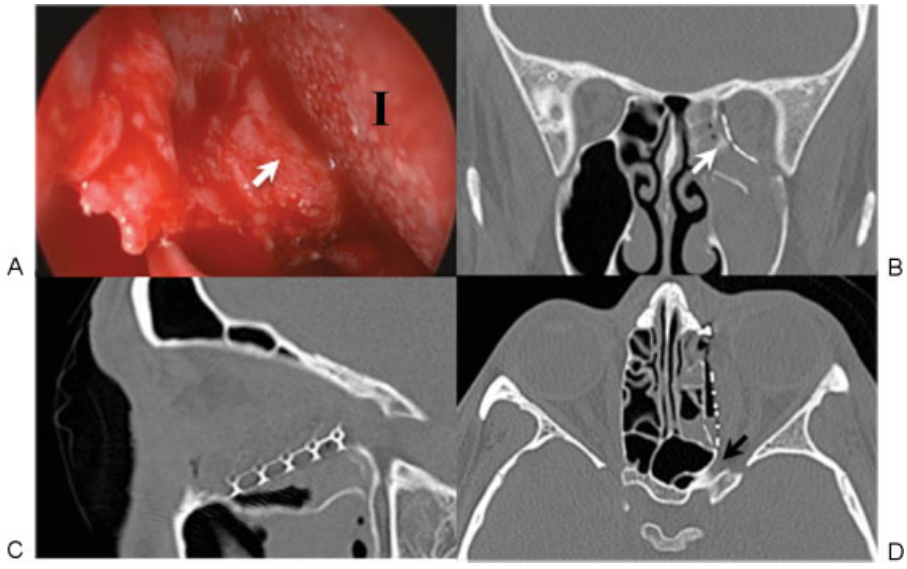

Figure 7 (A) Intraoperative endoscopy with corresponding postoperative computed tomography scan images (B, C, D). The camera was placed through the transcaruncular incision into the ethmoid sinus and used to visualize the posterior edge of the implant (I) as it was placed over the inferomedial bony ledge (white arrows in A and B). Although the medial wall fracture extended all the way to the optic foramen (black arrow in D), precise implant positioning was achieved without impinging on the optic nerve.

Acknowledgment

The authors thank Ms. Christy Landt, MS, for her assistance in performing statistical analysis for this study.

Disclaimer

The views presented in this article are those of the authors and do not represent the official position of Brooke Army Medical Center, the U.S. Army Medical Department, the Department of the Army, or the Department of Defense.

References

1 Dortzbach RK. Orbital floor fractures. Ophthal Plast Reconstr Surg 1985;1:149–151
2 Segrest DR, Dortzbach RK. Medial orbital wall fractures: complications and management. Ophthal Plast Reconstr Surg 1989;5: 75–80
3 Dutton JJ. Management of blow-out fractures of the orbital floor. Surv Ophthalmol 1991;35:279–280
4 Burnstine MA. Clinical recommendations for repair of orbital facial fractures. Curr Opin Ophthalmol 2003;14:236–240
5 Harris GJ. Orbital blow-out fractures: surgical timing and technique. Eye (Lond) 2006;20:1207–1212

6 Su GW, Harris GJ. Combined inferior and medial surgical approaches and overlapping thin implants for orbital floor and medial wall fractures. Ophthal Plast Reconstr Surg 2006;22: 420–423

7 Choi JC, Fleming JC, Aitken PA, Shore JW. Porous polyethylene channel implants: a modified porous polyethylene sheet implant designed for repairs of large and complex orbital wall fractures. Ophthal Plast Reconstr Surg 1999;15:56–66

8 Nunery WR, Tao JP, Johl S. Nylon foil "wraparound" repair of combined orbital floor and medial wall fractures. Ophthal Plast Reconstr Surg 2008;24:271–275

9 Schön R, Metzger MC, Zizelmann C, Weyer N, Schmelzeisen R. Individually preformed titanium mesh implants for a true-to-original repair of orbital fractures. Int J Oral Maxillofac Surg 2006;35:990–995

10 Scolozzi P, Momjian A, Heuberger J, et al. Accuracy and predictability in use of AO three-dimensionally preformed titanium mesh plates for posttraumatic orbital reconstruction: a pilot study. J Craniofac Surg 2009;20:1108–1113

11 Goldberg RA, Shorr N, Cohen MS. The medical orbital strut in the prevention of postdecompression dystopia in dysthyroid ophthalmopathy. Ophthal Plast Reconstr Surg 1992;8:32–34

12 Wright ED, Davidson J, Codere F, Desrosiers M. Endoscopic orbital decompression with preservation of an inferomedial bony strut: minimization of postoperative diplopia. J Otolaryngol 1999;28: 252–256

13 Kim JW, Goldberg RA, Shorr N. The inferomedial orbital strut: an anatomic and radiographic study. Ophthal Plast Reconstr Surg 2002;18:355–364

14 Lee HBH, Nunery WR. Orbital adherence syndrome secondary to titanium implant material. Ophthal Plast Reconstr Surg 2009; 25:33–36

15 Holck DEE, Dahl T, Foster JA, Ng JD. Internal orbital wall fracture repair using porous polyethylene/titanium mesh (MEDPOR TITAN) implants. MEDPOR TITAN White Paper; 2005

16 Garibaldi DC, Iliff NT, Grant MP, Merbs SL. Use of porous polyethylene with embedded titanium in orbital reconstruction: a review of 106 patients. Ophthal Plast Reconstr Surg 2007;23:439–444

17 Kahana A, Lucarelli MJ, Burkat CN, Dortzbach RK. Orbital fractures. In: Mallajosyula S, ed. Surgical Atlas of Orbital Disease. New York, NY: McGraw Hill 2009:220–243

18 Kim CY, Jeong BJ, Lee SY, Yoon JS. Comparison of surgical outcomes of large orbital fractures reconstructed with porous polyethylene channel and porous polyethylene titan barrier implants. Ophthal Plast Reconstr Surg 2012;28:176–180

19 McCord CD Jr, Moses JL. Exposure of the inferior orbit with fornix incision and lateral canthotomy. Ophthalmic Surg 1979;10: 53–63

20 Shore JW. The fornix approach to the inferior orbit. Adv Ophthalmic Plast Reconstr Surg 1987;6:377–385

21 Silkiss RZ, Carroll RP. Transconjunctival surgery. Ophthalmic Surg 1992;23:288–291

22 Appling WD, Patrinely JR, Salzer TA. Transconjunctival approach vs subciliary skin-muscle flap approach for orbital fracture repair. Arch Otolaryngol Head Neck Surg 1993;119:1000–1007

23 Shorr N, Baylis HI, Goldberg RA, Perry JD. Transcaruncular approach to the medial orbit and orbital apex. Ophthalmology 2000;107:1459–1463

24 Graham SM, Thomas RD, Carter KD, Nerad JA. The transcaruncular approach to the medial orbital wall. Laryngoscope 2002;112: 986–989

25 Kim S, Helen Lew M, Chung SH, Kook K, Juan Y, Lee S. Repair of medial orbital wall fracture: transcaruncular approach. Orbit 2005;24:1–9

26 Rodriguez J, Galan R, Forteza G, et al. Extended transcaruncular approach using detachment and repositioning of the inferior oblique muscle for the traumatic repair of the medial orbital wall. Craniomaxillofac Trauma Reconstr 2009;2:35–40

27 Lee CS, Yoon JS, Lee SY. Combined transconjunctival and transcaruncular approach for repair of large medial orbital wall fractures. Arch Ophthalmol 2009;127:291–296

28 Scolozzi P. Reconstruction of severe medial orbital wall fractures using titanium mesh plates placed using transcaruncular-transconjunctival approach: a successful combination of 2 techniques. J Oral Maxillofac Surg 2011;69:1415–1420

29 Metzger MC, Schön R, Tetzlaf R, et al. Topographical CT-data analysis of the human orbital floor. Int J Oral Maxillofac Surg 2007;36:45–53

30 Ploder O, Klug C, Voracek M, Burggasser G, Czerny C. Evaluation of computer-based area and volume measurement from coronal computed tomography scans in isolated blowout fractures of the orbital floor. J Oral Maxillofac Surg 2002;60:1267–1272, discussion 1273–1274

31 Ye J, Kook KH, Lee SY. Evaluation of computer-based volume measurement and porous polyethylene channel implants in reconstruction of large orbital wall fractures. Invest Ophthalmol Vis Sci 2006;47:509–513

32 Kwon J, Barrera JE, Jung TY, Most SP. Measurements of orbital volume change using computed tomography in isolated orbital blowout fractures. Arch Facial Plast Surg 2009;11:395–398